Estimation of the Thermodynamic Limit of Overheating for Bulk Water from Interfacial Properties

A.R. Imre[1,2*], A. Baranyai[3], U. K. Deiters[2], P.T. Kiss[3], T. Kraska[2]and S. E. Quiñones Cisneros[4]

1 HAS Centre for Energy Research, H-1525 Budapest, POB 49, Hungary

2 Institute for Physical Chemistry, University of Cologne, Luxemburger Str. 116, D-50939 Köln, Germany

3 Institute of Chemistry, Eötvös University, 1518 Budapest 112, P.O. Box 32, Budapest, Hungary

4 Instituto de Investigaciones en Materiales, Universidad Nacional Autónoma de México, Apdo. Postal 70-360, México D.F. 04510, México

* corresponding author, imre.attila@energia.mta.hu

ABSTRACT

The limit of overheating or expanding is an important property of liquids, which is relevant for the design and safety assessment of processes involving pressurized liquids. In this work, the thermodynamic stability limit – the so-called spinodal – of water is calculated by molecular dynamics computer simulation, using the molecular potential model of Baranyai and Kiss. The spinodal pressure is obtained from the maximal tangential pressure within a liquid–vapor interface layer. The results are compared to predictions of various equations of states. Based on these comparisons, a set of equations of state is identified which gives reliable results in the metastable (overheated or expanded) liquid region of water down to −55 MPa.

Keywords: overheating; stability limit; explosivity; equation of state; spinodal; boiling

International Journal of Thermophysics 09/2013; 34:2053–2064. DOI:10.1007/s10765-013-1518-8

1 Introduction

At ambient pressure, water is *usually* liquid between 0 and 100 °C; below that range, one can obtain solid phases (ice), while above that range lies the vapor phase (steam). But *unusual* behavior is possible, too: still at ambient pressure, water can be kept in the liquid state down to −42 °C and up to approximately 300 °C [1−4], giving a liquid range three and half times wider than the usual stable range. Outside the stable range, the liquid is metastable. This means that the liquid can be kept in this state for extended periods of time, but that external disturbances can cause it to freeze or boil; it may even freeze or boil at any moment without external disturbances, due to internal fluctuations.

The phase transition from a metastable state to a stable one can be very fast and drastic. Theoretically, the explosive boiling (also called flashing) of highly overheated water can release energy in the same order of magnitude as similar amount of TNT [5]. Unlike normal boiling, explosive boiling can happen within a fraction of a second. The phenomenon constitutes an operational hazard for equipment containing heated pressurized liquids: after a sudden accidental pressure loss or temperature increase, the liquid might reach a deeply metastable state and then relax by explosive boiling. LOCA (Loss of Coolant Accident) in pressurized water nuclear reactors [6] and BLEVE (Boiling Liquid Expanding Vapor Explosion, [7, 8]) in pressurized (liquified) gas tanks are two well known examples for violent and sudden boiling and the cause of many accidents. To minimize the risk of accidents, scientists and engineers dealing with pressurized heated liquids should be aware of the metastable region and know the properties of liquids in it.

An important property in this context is the limit of stability, i.e., the border between stable (including metastable) states and the unstable regions. There are three different kinds of limits: the spinodal, the homogeneous nucleation limit, and the heterogeneous nucleation limit [2, 3, 9-12]. The absolute limit is the thermodynamic limit (spinodal), where the compressibility turns from positive to negative. Obviously, systems with negative compressibility cannot be stable. When the immediate vicinity of the spinodal is reached, the phase transition cannot be delayed anymore: the metastable vapor has to turn into liquid, and the metastable liquid has to turn into vapor. Theoretically, spinodal states for pure fluids can be obtained easily from the equations of state; they correspond to extrema of $p(V)$ isotherms. Usually, relaxation from the

metastable state to stable one happens –- before reaching the spinodal –- by a different process (nucleation), but as an absolute limit, the spinodal is still very important.

Although in most cases the metastability will be terminated by boiling, initiated by homogeneous or heterogeneous nucleation [2, 12–15], the spinodal is important for two reasons. First, when the pressure drop or temperature increase is very fast, near-spinodal states can be reached before the nucleation takes place. Secondly, the homogeneous nucleation limit is sometimes very close to the spinodal (see for example in Ref. [15, 16]). Therefore, for a "conservative estimate" in safety calculations, the spinodal can be used for worst-scenario models [17]. This is especially true as *normal* boiling starts in a few places (nucleation centers) and then spreads to other parts of the liquid, whereas *spinodal* boiling occurs simultaneously all over the liquid [2], which is one of the reasons for its violent effect.

Another important field of application is volcanology. Liquid water or aqueous solutions can come into contact with hot magma and reach near-spinodal states, in which case explosive boiling may take place [5, 18], although in this case only the $p>0$ portion of the metastable region is relevant. The process called "steam explosion" in nuclear power plants – when a hot molten fuel drops into the cooling water – is similar and requires knowledge of the ultimate overheating limit [19].

The third application is the study of fluid inclusions in minerals. In some inclusions, the fluid can remain in an expanded liquid state (of the metastable region). The pressure of the liquid, either water or aqueous solutions, can be negative and, at low temperature, even reach the range of −60 to −140 MPa, as calculated from various reference equations of state for water [20−22]. The real spinodal should be at even lower pressures. These values differ considerably from the results of experiments where the pressure was measured directly [12, 13], where the estimated spinodal values for bulk water were above −50 MPa in the same temperature range. There are several reasons for these differences. An excellent overview was given by Caupin [23]. One of them is that an equation of state used outside its range of validity might produce artifacts [24]. For example, the IAPWS-95 EoS, which is a very reliable reference equation of state for water, was designed to be used only in the stable phases and down to a very minor metastability [25], certainly not below −5 MPa. Although recent investigations show that it might be good below that value [13], its accuracy and reliability can no longer be guaranteed.

From an engineering point of view, explosive boiling is not a purely thermodynamic problem; the propagation of heat, the contact between the wall and the liquid, and other factors are very important, particularly for the dynamics of this process [26]. But for conservative estimations of the limit of superheating, the knowledge of the location of the spinodal is necessary. In this paper, we propose some equations of state for water which are reasonably accurate in the metastable liquid region, at least down to a certain value. For this we will compare liquid−vapor spinodals predicted by several equations of state with results obtained with a novel computer simulation method. The proposed equation of state seems to be accurate concerning the prediction of the spinodal down to −55 MPa.

2 Spinodals by various equations of states

The spinodal state of a pure fluid is defined as the state at which it becomes mechanically unstable, i.e., at which the isothermal compressibility κ_T turns negative. If the fluid is modeled with a continuous and analytic equation of state, spinodal states correspond to the extrema of the pressure isotherms [27]. This is illustrated by Fig. 1a, which shows a subcritical isotherm of the van der Waals equation of state, computed for the temperature T_r = 0.8 T/T_c, where T_c is the critical temperature. The stable equilibrium phases were obtained with the Maxwell construction (area A = area B), see for example Ref. [28]; the horizontal line represents the vapor pressure. These calculations, as well as all other EoS-related calculations in this work, were performed with the *ThermoC* program package [29]; surface tension data were calculated with the Fluid Properties engine of NIST Chemistry Webbook [30]. The maximum of the isotherm is the vapor−liquid (VL) spinodal; this is the state at which an oversaturated vapor *has* to turn into liquid . The minimum is the liquid−vapor (LV) spinodal; here overheated or expanded liquid *must* boil and turn into vapor. In this work, the LV spinodal is considered.

Plotting the vapor pressures and the pressure extrema for a series of isotherms leads to Fig. 1b. The pressure maxima give rise to the VL spinodal curve, which starts at the critical point and approaches the abscissa with decreasing temperature. This spinodal curve always stays above the abscissa, as a vapor or gas cannot exist at negative pressure [2, 31]. The LV spinodal also starts at the critical point, but then runs towards negative pressures. Between the two

spinodal curves there is the vapor pressure curve, which also originates from the critical point and, since a gaseous phase is involved, has to remain at positive pressures. We should mention here that there are some EoSs for which $p<0$ values of the spinodal cannot be obtained. An example is the Dieterici equation of state [32]. Evidently, such EoS cannot describe deeply metastable liquids at negative pressure.

In Fig. 1b several regions can be identified:

1. Above the VL spinodal, one can find stable liquid only.
2. Between the vapor pressure curve and the VL spinodal, in the narrow, blade-like region, a stable liquid *or* an oversaturated vapor can be found (as in the cloud chambers used to detect ionizing particles [33]).
3. At the high-temperature side of the LV spinodal, but still at positive pressure, there is the stable vapor (or gas) region.
4. The region of metastable liquid technically can be divided into two parts: In the small triangular region below the vapor pressure curve, but above $p=0$, one can find stable vapor (steam) or overheated (metastable) liquid; this region can be reached either by stretching or by overheating a liquid. In the larger triangular region (below the $p=0$ line, but still above the LV spinodal) one can find metastable liquid only. Here a vapor or gas phase cannot exist, as negative pressure states are not allowed for gases [31]. This sub-region can be reached by stretching only. It should be noted that the properties of the metastable liquids in these two sub-regions are the same; merely the ways to reach them are different.
5. The region below the line on the high-temperature side of the LV spinodal, just below the region of stable vapor, is forbidden. No fluid phase can exist here, as a liquid would be unstable and a gas cannot exist at negative pressures. Only solid phases might exist in some part of this region, mainly towards low temperatures, as these can exist at pressures more negative than liquids [34, 35]; in this work, however, we will deal with fluid phases only. Incidentally, it is a common mistake to call this region the region of the unstable

liquid: there is no such thing as an unstable liquid: once the LV spinodal has been crossed, the liquid state ceases to exist.

Simple EoSs are usually not sufficient for accurate work. There are many EoSs which, if their parameters are fitted to the critical pressure and temperature, fail to match the experimental value for the critical compression factor, or predict a too narrow phase envelope (the density range between stable liquid and vapor phases). In contrast to these, reference equations of state can reproduce the thermodynamic data of fluids including their phase behaviour within the experimental uncertainty. They are, however, mathematically more complicated, perhaps less elegant, and no physical interpretation can be given for their terms. The best available reference EoS for water was developed by Wagner and Pruß [25]. It is also known as the IAPWS-95 EoS, because it was adopted by the International Association for the Properties of Water and Steam. In their paper, Wagner and Pruß warn against using their EoS far away from the stable region, because only thermodynamic data of stable states were used for the fitting of the parameters of their EoS. On the other hand, if an EoS is good over a very wide range of pressure down to almost p=0, one may expect that it is reasonably accurate slightly below zero. Indeed, Caupin and his co-workers [13] proved that the liquid–vapor spinodal derived from this EoS is fairly accurate down to −26 MPa (which corresponds to a reduced temperature of approximately 0.86). In this work, we wish to extend their work and show that the limit of applicability of the IAPWS-95 EoS is even lower, but also warn against using this EoS indiscriminately beyond that limit.

Reference equation of states differs from theoretical EoS in several ways; one of them is the existence of unrealistic isotherms with more than two extrema. Figures 2a and b show an isotherm (T_r = 0.8, as in Fig. 1) of the IAPWS EoS. The isotherm exhibits a well-developed maximum and minimum, but these extrema are much too large to be the real spinodals: the maximum (nicknamed “Himalaya” in the diagram) occurs at +3500 GPa and the minimum (“Mariana Trench”) at −1950 GPa, which is well beyond the stability limits of a solid single crystal [34] by more than one order of magnitude. A magnification of the pressure region around p=0 (Fig. 2b) reveals the existence of an additional smaller minimum and maximum, i.e., this isotherm has four extrema. The original Wagner and Pruß paper mentions the occurrence of the extra extrema and recommends using the two outermost ones only. But from Fig. 2b – especially

when compared to Fig. 1a – one can see that the presence of those gigantic peaks strongly deforms the two small peaks, which are much narrower than in the case of the cubic EoS.

Figure 3 contains the LV spinodal and the vapor pressure curve, as predicted by various EoS for water. These EoS are the first cubic equation of state, namely the original van der Waals equation (vdW) [35], the Redlich−Kwong EoS (RK) [37], which can be used with some success to predict the overheating of some organic compounds at atmospheric pressure [8], the Deiters equation (D) [38], and three noncubic EoS, namely the already mentioned IAPWS-95 [25], the GERG-2004 natural gas reference equation (GERG), which is a set of EoS for the compounds found in light natural gas including water [39], and finally the Xiang–Deiters EoS (XD), which is based on a four-parameter corresponding-states approach [40]. As can be seen, the spinodals differ not only quantitatively, but qualitatively, too. For some EoS, the spinodal pressure decreases with temperature monotonically [9], while for others it passes through a minimum. The latter behavior is the so-called re-entrant spinodal scenario [2, 41].

3 Calculation of Spinodals by Computer Simulation

It has been known for a while that the fluid at a vapor−liquid interfacial region has some similarities to the metastable fluid, see Refs. [42−44] and references therein. The similarity is not only qualitative but, as proposed previously [44, 45], the bulk spinodal can be estimated with a fairly good accuracy from the minimal value of the tangential pressure component of the liquid−vapor interface layer, $p_{T,min}(T)$, in the following way:

(1)

Here $p_{sp}(T)$ and $p_N(T)$ are the temperature-dependent spinodal pressure and the normal component of the interfacial pressure. $p_N(T)$ is equal to the equilibrium vapor pressure ($p_{vap}(T)$ plus the hydrostatic pressure, which is practically zero in our case). The factor c is 3/2, it turns the 2D surface property into a 3D bulk property [45].

This method has been successfully applied to model fluids such as a Lennard-Jones fluid and the Shan−Chen fluid (a simple fluid used in lattice-Boltzmann simulations) [45] as well as to

carbon dioxide [46]. A modified version, where $p_{T,min}(T)$ is estimated from measurable interface properties with some extra assumptions about the shape of the pressure profile, has been used for ^{3}He and ^{4}He [47]. Furthermore, some preliminary results for low-temperature water have already been reported [48].

In this work, we have modeled the interface layer of water by molecular dynamics simulation using an interaction potential recently proposed by Baranyai and Kiss [49]. This interaction potential is rigid and uses three Gaussian charge distributions as well as a field-dependent polarizability. It had originally been fitted to experimental data of ambient water and hexagonal ice, but also gives good predictions for the energy and structure of gas-phase clusters, the temperature dependence of the second virial coefficient, and the equilibrium properties along the vapor–liquid coexistence curve. The predicted critical properties are close to the experimental values [50].

The interface simulations were performed for several temperatures between 440 and 570 K in a tetragonal simulation box (28 Å × 28 Å × 120 Å) containing 1000 molecules, the majority of which forming a liquid layer approximately at $z = \pm 20$ Å. In the x and y directions, periodic boundary conditions were employed. After equilibration, the averages were collected every 2 ns. For the technical details of the pressure calculation with Ewald summation and polarizable models, see Ref. [51]; for simulated water properties, see Table 1 and Ref. 50. The z-dependence of the normal and tangential elements of the pressure tensor was calculated following Irving and Kirkwood, [52]. A typical tangential pressure profile of a liquid film (T = 460 K) can be seen in Fig. 4, showing well-developed minima for the the p_T component.

4 Results and Discussions

The simulation results for the LV spinodal of water are displayed in Fig. 5. Errors can be estimated from Equation 1, using the errors of normal and tangential pressure components, giving values between 0.1 and 0.8 MPa at the low and high temperature limit, respectively. These errors cannot be seen in Fig. 5, the error bars being smaller than the symbols. The LV spinodal can be represented with a second-order polynomial, as:

$$p_{r\text{-}sp}(\mathrm{LV}) = -24.0(\pm 2.2)\, T_r^2 + 60.9(\pm 3.7)\, T_r - 35.9(\pm 1.6) \qquad (2)$$

where $p_r = p / p_c$ denotes the reduced pressure. Equation 2 is valid in the reduced temperature range 0.68–1, R^2=0.9985.

Fig. 5 also contains the predictions of three equations of state, namely IAPWS, GERG, and XD. As already shown in Fig. 3, these three EoS predict very similar spinodals down to p_r=−2.5 (approximately −55 MPa). Now it turns out that the predictions agree within 5 % with the simulation results. The differences between these and the EoS predictions would look slightly larger in a real pressure–temperature representation, as the Baranyai–Kiss model underestimates the critical pressure and temperature of water (giving 623 K and 22.7 MPa, instead of 647 K and 22.06 MPa), but still can be considered acceptable. The underestimation disappears and the equilibrium and stability lines would be also realistic by using reduced quantities.

The spinodals generated from the other EoS widely differ from the simulation results, and therefore have been omitted in Fig. 5. These equations (van der Waals, Redlick-Kwong and Deiters) cannot be recommended for the calculation of water spinodals.

Unfortunately, in the low-temperature region (where re-entrant behavior might be seen), the interface thickness in the simulations becomes so small (2–3 molecules wide) that the interfacial tangential pressure profile cannot be obtained properly with the present method. Therefore we cannot say at present which type of the spinodal – re-entrant or monotonic – is supported by our model.

Down to p_r = −2.5 (approximately −55 MPa), the IAPWS, GERG, and XD equations are quite reliable; the XD and GERG spinodals seem to be better than the IAPWS one. Below −55 MPa, the three EoS spinodals deviate more and more from the simulation results, although the IAPWS spinodal seems to be slightly better.

In general, we can conclude that from −55 MPa up to the critical point, the spinodal curves obtained with the GERG and Xiang–Deiters equations agree with the computer simulation results obtained with the interface method of Imre and Kraska, using the Baranyai–Kiss model (IK-BK), within the error caused by the simulation noise in the tangential pressure.

The deviation of the IAPWS-95 spinodal is slightly worse, usually twice the deviation of the other EoS, but still good in comparison with other equations of state.

The prediction of metastable states from the equations of state is an extrapolation and naturally uncertain. Obviously, the GERG, Xiang–Deiters, or the IAPWS-95 equations ***alone*** might conceivably give false spinodals. But the fact that these – mathematically different – equations predict very similar spinodals argues for the validity of the predictions. That practically the same spinodal could be obtained with a totally different method, namely computer simulation, is another strong argument for its reliability.

As the predictions of several independent methods agree within a narrow error margin, we conclude that the real spinodal of water lies in the very close vicinity of the predicted curves. We therefore recommend using the GERG, Xiang–Deiters, or IAPWS-95 equations of state for the calculation of the properties of metastable water in the high-temperature region down to −55 MPa. Therefore their use can be recommended for conservative estimates for some calculations – such as total energy release – during explosive boiling.

Acknowledgments

Part of this project was financed by the Hungarian Atomic Energy Authority. A.R. Imre's stay in Germany was financed by the German Humboldt Foundation. A. Baranyai gratefully acknowledges the support of OTKA grant K84382.

References

1. C.T. Avedisian, J. Phys. Chem. Ref. Data, **14**, 695 (1985)

2. P.G. Debenedetti, *Metastable Liquids: Concepts and Principles* (Princeton University Press, Princeton, NJ., 1996)

3. A.R. Imre, H.J. Maris, P.R. Williams (Eds.) *Liquids under Negative Pressure* (NATO Science Series, Kluwer, Dordrecht, 2002)

4. P.V. Skripov, A.P. Skripov, Int. J. Thermophys. **31**, 816 (2010)

5 R. Thiéry, L. Mercury, J. Geophys. Res. **114**, B05205 (2009)

6. A. Poullikkas, Progr. Nucl. Energ. **42**, 3 (2003)

7. G.A. Pinhasi, A. Ullman, A. Dayan, Rev. Chem. Eng. **21**, 133 (2005)

8. T. Abbasi, S.A. Abbasi, J. Loss Prevent. Process Ind. **20**, 165 (2007)

9. V. P. Skripov, *Metastable Liquids* (Wiley, New York, 1974)

10. V.G., Baidakov, Sov. Tech. Rev. B. Therm. Phys. **5**, 1 (1994)

11. S.B. Kiselev, Physica A **269**, 252 (1999)

12. E. Herbert, S. Balibar, F. Caupin, Phys. Rev. E **74**, 041603 (2006)

13 K. Davitt, A. Arvengas, F. Caupin, Europhys. Lett. **90**, 16002 (2010)

14 J.H. Lienhard, A. Karimi, J. Heat Transfer **103**, 61 (1981)

15. C.E. Cordeiro, J.B. Silva, S.M. de Oliveira, A. Delfino, J.S. Saa Martins, Int. J. Thermophys. **28**, 1267 (2007)

16 M.N. Hasan, M. Monde, Y. Mitsutake, Int. J. Heat Mass Transfer, **54**, 3226 (2011)

17 N. Shamsundar, J.H. Lienhard, Nucl. Eng. Design **141**, 269 (1993)

18. R. Thiéry, L. Mercury, J. Sol. Chem. **38,** 893 (2009)

19. J. Lamome, R. Meignen, Nucl. Eng. Design **238**, 3445 (2008)

20. E. Roedder, Science **155**, 1413 (1967)

21. J.L. Green, D.J. Durben, G.H. Wolf, C.A. Angell, Science **249**, 649 (1990)

22. K.I. Shmulovich, L. Mercury, R. Thiéry, C. Ramboz, M. El Mekki, Geochim. Cosmochim. Acta **73**, 2457 (2009)

23. F. Caupin, *From helium to water: capillarity and metastability in two exceptional liquids*, Habilitation thesis (École Normale Supérieure, Département de Physique, Paris, France, 2009)

24. I. Polishuk, J. Supercrit. Fluids **58**, 204 (2011)

25. W. Wagner, A. Pruß, J. Phys. Chem. Ref. Data **31**, 387 (2002)

26. M.N. Hasan, M. Monde, Y. Mitsutake, Int. J. Heat Mass Transfer **54**, 2844 (2011)

27. T. Kraska, Ind. Eng. Chem. Res. **43**, 6213 (2004)

28. U.K. Deiters, T. Kraska, *High-Pressure Fluid-Phase Equilibria — Phenomenology and Computation* (Elsevier, Amsterdam, 2012)

29. U.K. Deiters, *ThermoC* project website, http://thermoc.uni-koeln.de/ (2006)

30. NIST Chemistry Webbook, http://webbook.nist.gov/chemistry/ (2011)

31. A. Imre, K. Martinás, L.P.N. Rebelo, J. Non-Equilib. Thermodyn. **23**, 351 (1998)

32. I. Polishuk, R. Gonzalez, J.H. Vera, H. Segura, Phys. Chem. Chem. Phys. **6**, 5189 (2004)

33. N.N. Das Gupta, S.K. Ghosh., Rev. Mod. Phys. **18**, 225 (1946)

34. P. McMillan, Nature Mater. **1**, 19 (2002)

35. A.R. Imre, A. Drozd-Rzoska, T. Kraska, S.J. Rzoska, K.W. Wojciechowski, J. Phys. Cond. Matter. **20**, 244104 (2008)

36. J. D. van der Waals, in: *Nobel Lectures—Physics 1901–1921* (S. Lundqvist, ed.) (Nobel Foundation, Stockholm 1998) p.254

37. O. Redlich, J.N.S. Kwong, Chem. Rev. **44**, 233 (1949)

38. U.K. Deiters, Chem. Eng. Sci. **36**, 1139, 1146 (1981)

39. O. Kunz, R. Klimeck, W. Wagner, M. Jaeschke, *The GERG-2004 Wide-Range Reference Equation of State for Natural Gases and other Mixtures*, GERG Technical Monograph 15 (European Gas Research Group (GERG), VDI-Verlag, Düsseldorf, 2007)

40. H.-W. Xiang, U.K. Deiters, Chem. Eng. Sci. **63**, 1490 (2007)

41. R.J. Speedy, J. Phys. Chem. **86**, 982 (1982)

42. G. Bakker, Z. Phys. Chem. **90**, 359 (1915)

43. F. Caupin, Phys. Rev. E. **71**, 051605 (2005)

44. A.R. Imre, T. Kraska, Fluid Phase Equilib. **284**, 31 (2009)

45. A.R., Imre, G. Mayer, G. Házi, R. Rozas, T. Kraska, J. Chem. Phys. **128**, 114708 (2008)

46. F. Römer, A.R. Imre, T. Kraska, J. Phys. Chem. B **113**, 4688 (2009)

47. A.R. Imre, T. Kraska, Physica B **403**, 3663 (2008)

48. A.R. Imre, G. Házi, T. Kraska, in NATO Science Series: *Metastable Systems under Pressure* (Eds.: S.J. Rzoska, A. Drozd-Rzoska, V. Mazur) (Springer, Dordrecht, 2009) p271

48. A. Baranyai, P.T. Kiss, J. Chem. Phys. **135,** 234110 (2011)

50. P.T. Kiss, M. Darvas, A. Baranyai, P. Jedlovszky, J. Chem. Phys. **136**, 114706 (2012)

51. P.T. Kiss, A. Baranyai, J. Chem. Phys. **136**, 104109 (2012)

52. J. H. Irving, J. G. Kirkwood, J. Chem. Phys. **18**, 817 (1950)

T_r	Source	ρ_L (g·cm^{-3})	ρ_V (g·cm^{-3})	P_N or P_{vap} (bar)	P_T (bar)	γ (mN·m^{-1})	ΔH_{vap} (kJ·mol^{-1})
0.690	this calculation	0.8894	0.0040	11.2 ± 0.1	−46.1 ± 0.5	43.1	36.65
	reference	*0.8939*	*0.0045*	*8.6*	-	*43.6*	*36.70*
0.722	this calculation	0.8674	0.0062	16.9 ± 0.2	−35.6 ± 0.3	39.6	35.26
	reference	*0.8714*	*0.0070*	*13.7*	-	*39.0*	*35.35*
0.754	this calculation	0.8411	0.0102	24.0 ± 0.2	−22.0 ± 0.6	34.6	33.79
	reference	*0.8466*	*0.0106*	*21.0*	-	*34.2*	*33.85*
0.784	this calculation	0.8134	0.0140	35.7 ± 0.7	−6.7 ± 0.5	31.9	31.74
	reference	*0.8193*	*0.0155*	*31.0*	-	*29.4*	*32.17*
0.819	this calculation	0.7813	0.0219	52.0 ± 1.7	14.0 ± 0.6	28.5	29.42
	reference	*0.7891*	*0.0223*	*44.3*	-	*24.5*	*30.28*
0.851	this calculation	0.7426	0.0331	68.7 ± 1.5	37.5 ± 0.7	23.5	28.48
	reference	*0.7551*	*0.0317*	*61.5*	-	*19.6*	*28.11*
0.883	this calculation	0.7008	0.0510	97.8 ± 1.4	69.2 ± 1.8	21.5	24.02
	reference	*0.7161*	*0.0447*	*83.5*	-	*14.8*	*25.57*
0.915	this calculation	0.6487	0.0755	129.5 ± 2.1	106.2 ± 1.9	17.5	-
	reference	*0.6699*	*0.0634*	*111.0*	-	*10.1*	-

Table 1: Vapor–liquid phase equilibrium properties of simulated water, compared to reference values (printed in *italics* for better visibility) calculated with ThermoC [29] by using the IAPWS EoS [25] (except for surface tension, which was taken from the NIST Webbook [30]).

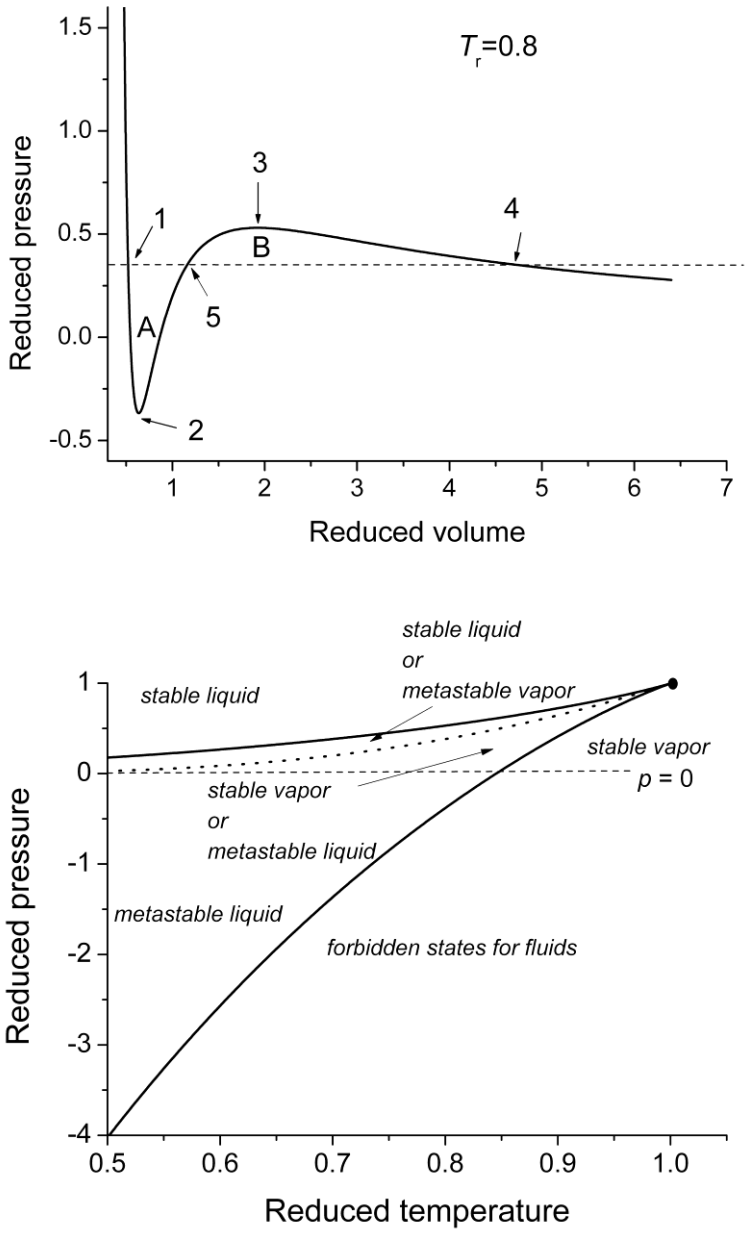

Figure 1: (a) Sub-critical isotherm of the van der Waals equation of state at a reduced temperature of 0.8 (solid line). ----: Maxwell construction (area A=area B) to obtain equilibrium liquid (1) and vapor (4) phases; (2): liquid–vapor spinodal, (3): vapor–liquid spinodal. (b) Corresponding pressure–temperature diagram showing liquid–vapor (lower solid line) and vapor–liquid (upper solid line) spinodals. ·····: vapor pressure curve, ●: critical point

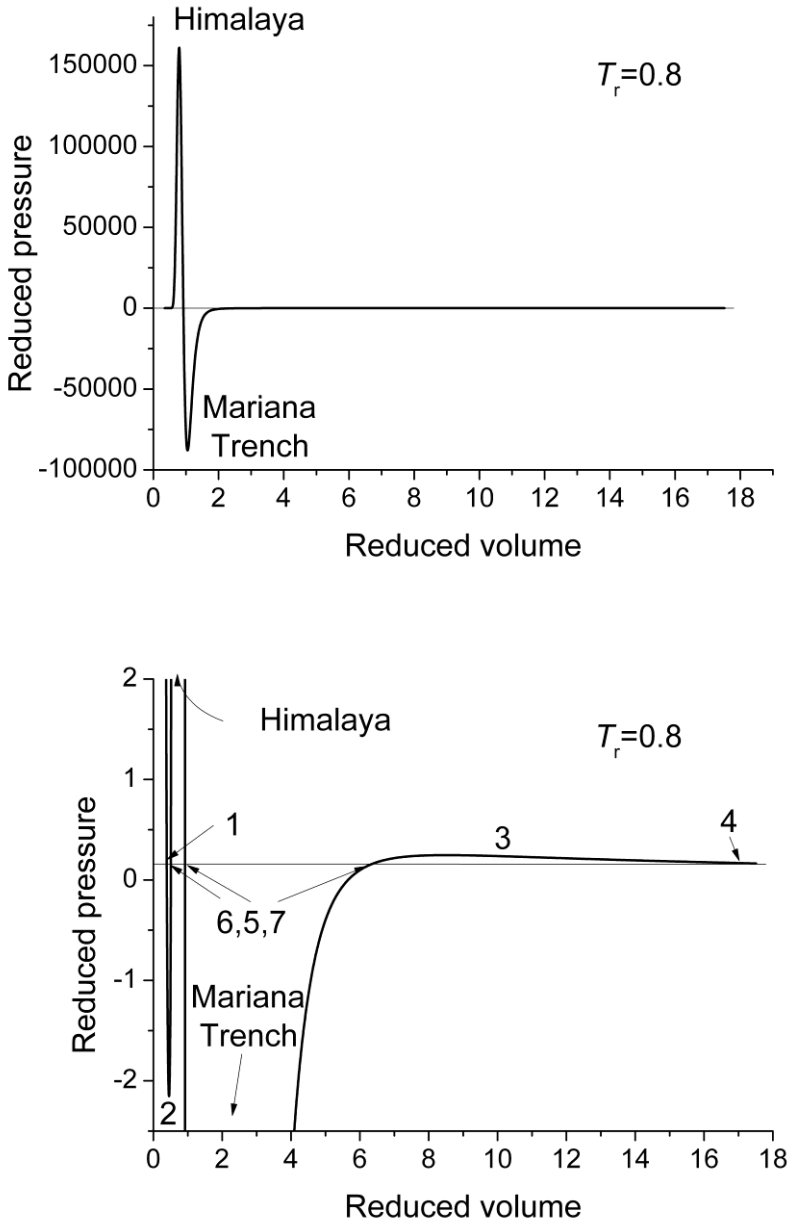

Figure 2: Pressure isotherm at T_r = 0.8 of the IAPWS EoS at two different ordinate scalings. (a) Overview showing the two spinodal-like extrema ("Himalaya" with approximately 3500 GPa height and "Mariana Trench" with approximately −1950 GPa depth; with some other reference EoSs even more extrema can occur). These artifacts are one of the main reasons for not to using a reference EoS outside of its range of validity. (b) Magnification of the low-pressure region, revealing the real spinodal states (2) and (3); (1): stable liquid, (4): stable vapor, (5–7): unphysical states

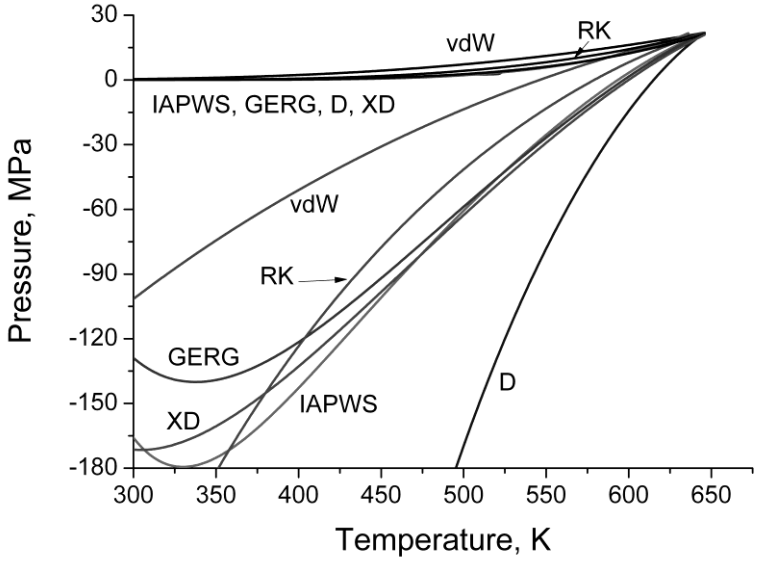

Figure 3. Comparison of liquid–vapor spinodals and vapor pressure curves obtained from various equations of states. See the text for an explanation of the abbreviations

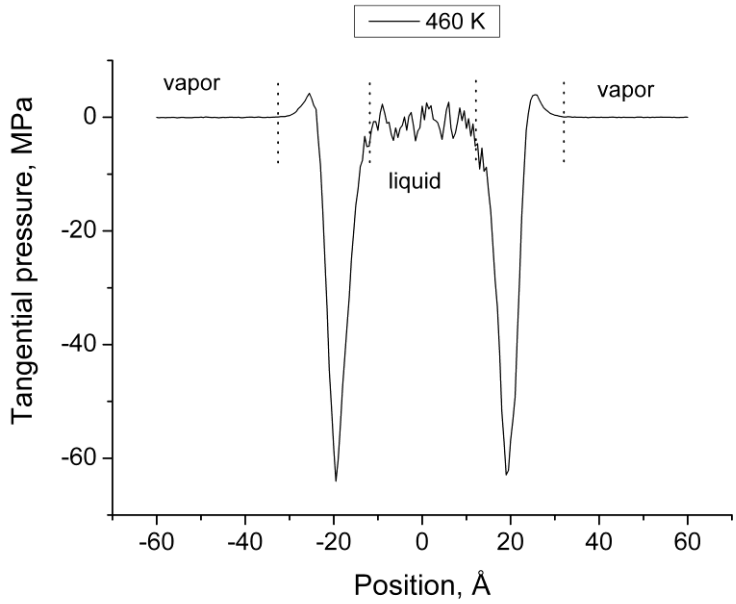

Figure 4. Tangential pressure components in a liquid film from an MD simulation at 460 K. Dotted lines mark the extent of vapor, liquid and interfacial regions

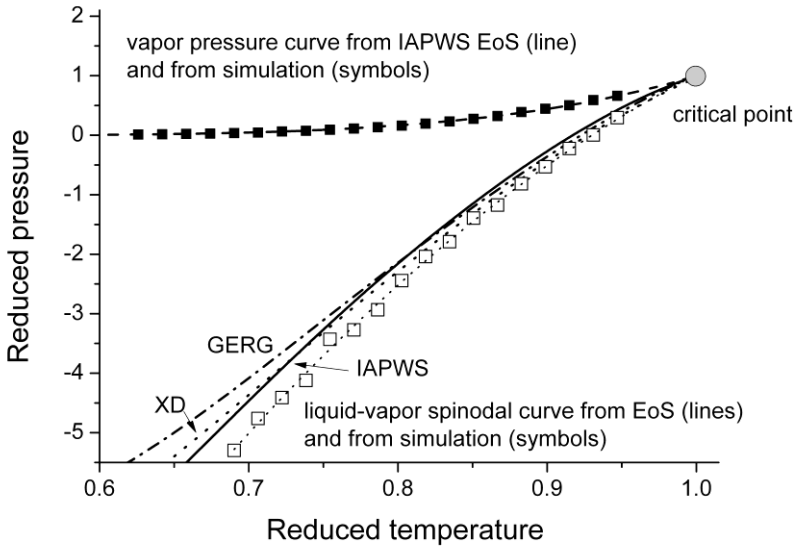

Figure 5. Phase diagram of fluid water at high temperatures. Symbols: MD simulation results (IK-BK, this work): ■: vapor pressure curve, □: LV spinodal; ----: vapor pressure curve calculated from the IAPWS EoS; other curves: LV spinodals: —: IAPWS EoS, - - -: XD EoS, –·–·–: LV GERG EoS, ·····: parabolic fit of the MD-data, Eq. 2